Impact of vector new physics couplings on $B_s \to (K,K^*)\tau\nu$ and $B \to \pi\tau\nu$ decays

N Rajeev* and Rupak Dutta†
National Institute of Technology Silchar, Silchar 788010, India

(Received 25 August 2018; published 19 September 2018)

Experimental measurements of R_D, R_{D^*} and $R_{J/\Psi}$ in $B \to (D, D^*)l\nu$ and $B_c \to J/\Psi l\nu$ decays mediated via $b \to c l\nu$ charged current interactions deviate from standard model prediction by 2.3σ, 3.0σ and 1.3σ, respectively. In addition, a deviation of 1.5σ from the standard model prediction has been witnessed in $\mathcal{B}(B \to \tau\nu)$ mediated via $b \to u l\nu$ charged current interactions as well. Motivated by the anomalies present in B and B_c meson decays, we analyze the corresponding $B_s \to (K, K^*)\tau\nu$ and $B \to \pi\tau\nu$ semileptonic decays within the standard model and beyond. We use an effective field theory formalism in which $b \to c$ and $b \to u$ semileptonic decays are assumed to exhibit similar new physics patterns. We give the predictions of various observables such as the branching fractions, ratio of branching ratios, lepton side forward backward asymmetry, lepton polarization fraction and convexity parameter for $B_s \to (K, K^*)\tau\nu$ and $B \to \pi\tau\nu$ decay channels within the standard model and within various new physics scenarios.

DOI: 10.1103/PhysRevD.98.055024

I. INTRODUCTION

The electroweak interactions which are mediated via Z^0 and $W^{\pm}$ bosons are categorized into flavor changing neutral current and charged current interactions. Deviations from the standard model (SM) predictions are observed not only in decays mediated via the $b \to (c, u)$ charged current processes but also in decays mediated via the $b \to s$ neutral current process. Most reliable measurements in charged current interactions include R_D, R_{D^*} and $R_{J/\Psi}$, where

$$R_{D^{(*)}} = \frac{\mathcal{B}(B \to D^{(*)}\tau\nu)}{\mathcal{B}(B \to D^{(*)}l\nu)}, \qquad R_{J/\Psi} = \frac{\mathcal{B}(B_c \to J/\Psi\tau\nu)}{\mathcal{B}(B_c \to J/\Psi l\nu)}. \tag{1}$$

Based on lattice calculations of Refs. [1,2], the SM predictions for R_D are 0.299 ± 0.011 and 0.300 ± 0.008, respectively. Combining the two lattice results, the value of R_D was reported to be 0.300 ± 0.008 by the FLAG working group [3]. A more accurate prediction of $R_D = 0.299 \pm 0.003$ was reported in Ref. [4] with the experimental form factor of $B \to Dl\nu$ from *BABAR* and Belle. Similar SM predictions were reported very recently by many groups. We refer to Refs. [5–7] for the details. The first SM prediction of $R_{D^*} = 0.252 \pm 0.003$ was reported in Ref. [8]. However, various new calculations of R_{D^*} are now available. Based on the calculations performed in Refs. [5,6,9], the arithmetic average was reported to be $R_{D^*} = 0.258 \pm 0.005$. Although the range for $R_{J/\Psi}$ was reported to be [0.25, 0.29] obtained using different form factors [10–12], very recently in Ref. [13], the authors have reported the new bound of [0.20, 0.39] for $R_{J/\Psi}$ at 95% confidence level. On the other hand, the average experimental values reported by HFLAG are $0.407 \pm 0.039 \pm 0.024$ and $0.304 \pm 0.013 \pm 0.007$ for R_D and R_{D^*} measured from *BABAR* [14], BELLE [15–17], LHCb [18] and $0.71 \pm 0.17 \pm 0.18$ for $R_{J/\Psi}$ from LHCb [19] measurement. This amounts to a combined deviation of around 3.78σ in R_D and R_{D^*} [20] and around 1.3σ in $R_{J/\Psi}$ from the SM expectations. Similarly, discrepancy between the measured value and the SM value has been observed in the $b \to u$ quark level transition decays as well. The average value of the branching ratio (BR) $\mathcal{B}(B \to \tau\nu) = (10.9 \pm 2.4) \times 10^{-5}$ reported in Ref. [21] from *BABAR* [22,23] and Belle [24,25] measurements is not in good agreement with the SM expectations [26–28]. However, the measured value of $\mathcal{B}(B \to \pi l\nu) = (14.5 \pm 0.5) \times 10^{-5}$ from BELLE [29–31] and *BABAR* [32–36] is consistent with its SM counterpart. The SM prediction, however, depends on not very well known CKM matrix element $|V_{ub}|$ and various meson to meson transition form factors. We define an observable in which the $|V_{ub}|$ dependency cancels in the ratio. That is

*rajeev@rs.phy.student.nits.ac.in
†rupak@phy.nits.ac.in

$$R_\pi^l = \frac{\tau_{B^0}}{\tau_{B^-}} \frac{\mathcal{B}(B \to \tau\nu)}{\mathcal{B}(B \to \pi l\nu)}, \tag{2}$$

where τ_{B^0} and τ_{B^-} are the lifetime of B^0 and B^- mesons. Using the measured values of $\mathcal{B}(B \to \tau\nu)$, $\mathcal{B}(B \to \pi l\nu)$ and the direct measurement of the ratio $\tau_{B^0}/\tau_{B^-} = 1.076 \pm 0.004$ [21], we get $R_\pi^l = 0.698 \pm 0.155$. In the SM, we obtain $R_\pi^l = 0.566$. This clearly shows a mild deviation from SM prediction. We also consider another useful observable which is potentially sensitive to new physics (NP), i.e.,

$$R_\pi = \frac{\mathcal{B}(B \to \pi\tau\nu)}{\mathcal{B}(B \to \pi l\nu)}. \tag{3}$$

In the SM, we obtain $R_\pi = 0.641$. Again, a naive estimate would give $R_\pi < 1.784$ using the present world average of $\mathcal{B}(B \to \pi l\nu) = (1.45 \pm 0.05) \times 10^{-4}$ [21] and the upper limit on $\mathcal{B}(B \to \pi\tau\nu) < 2.5 \times 10^{-4}$ reported by Belle Collaboration [37]. Similarly, by considering the branching fraction of $B \to \pi\tau\nu$ [37] and $\mathcal{B}(B \to \pi l\nu)$ [21], $R_\pi = 1.05 \pm 0.51$ was obtained in Ref. [38]. These indirect hints of existence of NP led the physics community to look for various NP scenarios. There exists various model-dependent and model-independent analysis in the literature in order to explain these anomalies, details of which can be found in Refs. [39–89].

In this paper, we are mainly interested in discussing the NP effects in $B_s \to (K, K^*)\tau\nu$ and $B \to \pi\tau\nu$ semileptonic decays mediated via $b \to u\tau\nu$ charged current interactions. Within the SM, the branching ratio and ratio of branching ratios of $B_s \to (K, K^*)\tau\nu$ and $B \to \pi\tau\nu$ decays have been studied extensively by various authors [90–96]. Very recently, in Ref. [97], the authors have performed a model-independent analysis of NP effects in $B_s \to (K, K^*)\tau\nu$ decays using the experimental constraints coming from the $B \to \tau\nu$ channel. Similarly, in Ref. [98] the authors have studied the $B_s \to (K, K^*)\tau\nu$ decay modes using the form factors obtained from the covarient light-front quark model. Our main aim is to study the implication of R_D, R_{D^*}, $R_{J/\Psi}$, and R_π^l anomalies in $B_s \to (K, K^*)\tau\nu$ and $B \to \pi\tau\nu$ semileptonic decays in a model-dependent way. To this end, we use an effective theory formalism in the presence of NP and perform a combined analysis of $b \to u$ and $b \to c$ semileptonic decays. This is where we differ significantly from Refs. [97,98]. Again, for various meson to meson transition form factors, we use very recent lattice QCD results of Refs. [94–96]. More importantly, we give the first prediction of various observables such as τ polarization fraction and convexity parameter for $B_s \to (K, K^*)\tau\nu$ and $B \to \pi\tau\nu$ decays within the SM and within various NP scenarios.

The present discussion in this paper proceeds as follows. In Sec. II, we first report the most general effective Lagrangian governing the $b \to (u, c)l\nu$ weak decays in the presence of NP. We also report all the relevant formulas corresponding to the various meson to meson form factors in this section. The relevant expressions for all the observables in the presence of vector NP couplings obtained using helicity formalism are reported in Sec. II. In Sec. III, we report the results pertaining to all the observables within the SM and within various NP scenarios. Finally we conclude with a brief summary of our results in Sec. IV.

II. METHODOLOGY

The most general effective Lagrangian for $b \to q'l\nu$ transition decays which includes both SM and beyond SM contributions is of the form [99,100]

$$\mathcal{L}_{\text{eff}} = -\frac{4G_F V_{q'b}}{\sqrt{2}} \Big(\mathcal{O}_{V_L} + \sum_{W=S_i,V_i,T_L} \delta_{\tau l} W \mathcal{O}_W + \sum_{\tilde{W}=\tilde{S}_i,\tilde{V}_i,\tilde{T}_R} \delta_{\tau l} \tilde{W} \tilde{\mathcal{O}}_{\tilde{W}} \Big), \tag{4}$$

where q' denotes a u quark or a c quark and $V_{q'b}$ is the relevant CKM matrix element. The four fermion operators $\mathcal{O}_W$ and $\tilde{\mathcal{O}}_{\tilde{W}}$ are defined as

$$\begin{aligned}
\mathcal{O}_{V_i} &= (\bar{q}'\gamma^\mu P_i b)(\bar{l}\gamma_\mu P_L \nu_l), \\
\tilde{\mathcal{O}}_{\tilde{V}_i} &= (\bar{q}'\gamma^\mu P_R b)(\bar{l}\gamma_\mu P_i \nu_l), \\
\mathcal{O}_{S_i} &= (\bar{q}' P_i b)(\bar{l} P_L \nu_l), \\
\tilde{\mathcal{O}}_{\tilde{S}_i} &= (\bar{q}' P_R b)(\bar{l} P_i \nu_l), \\
\mathcal{O}_{T_L} &= (\bar{q}'\sigma^{\mu\nu} P_L b)(\bar{l}\sigma_{\mu\nu} P_L \nu_l), \\
\tilde{\mathcal{O}}_{\tilde{T}_R} &= (\bar{q}'\sigma^{\mu\nu} P_R b)(\bar{l}\sigma_{\mu\nu} P_R \nu_l).
\end{aligned} \tag{5}$$

Here $i = L$, R and $\sigma_{\mu\nu} = i[\gamma_\mu, \gamma_\nu]/2$. The left and right projection are defined by $P_{L,R} = (1 \mp \gamma_5)/2$. We note that W and $\tilde{W}$ represent the complex Wilson coefficients (WCs) of NP contribution due to left handed and right handed neutrino interactions, respectively. We assume that the NP couples to u and c quarks with equal stregth; i.e., the WCs W and $\tilde{W}$ are quark flavor universal. The $\delta_{\tau l}$ restricts the NP effects only to the τ mode. Assuming the WCs to be real and considering NP contributions from the vector-type NP couplings alone, the effective Lagrangian can be written as [61]

$$\begin{aligned}
\mathcal{L}_{\text{eff}} = -\frac{G_F}{\sqrt{2}} V_{q'b} \{ & G_V \bar{l}\gamma_\mu (1-\gamma_5)\nu_l \bar{q}'\gamma^\mu b \\
& - G_A \bar{l}\gamma_\mu (1-\gamma_5)\nu_l \bar{q}'\gamma^\mu\gamma_5 b + \tilde{G}_V \bar{l}\gamma_\mu (1+\gamma_5)\nu_l \bar{q}'\gamma^\mu b \\
& - \tilde{G}_A \bar{l}\gamma_\mu (1+\gamma_5)\nu_l \bar{q}'\gamma^\mu\gamma_5 b \} + \text{H.c.},
\end{aligned} \tag{6}$$

where

$$\begin{aligned}
G_V &= 1 + V_L + V_R, \qquad G_A = 1 + V_L - V_R, \\
\tilde{G}_V &= \tilde{V}_L + \tilde{V}_R, \qquad \tilde{G}_A = \tilde{V}_L - \tilde{V}_R.
\end{aligned} \tag{7}$$

Using the effective Lagrangian of Eq. (6), the matrix element of the semileptonic decays $B \to (P, V) l\nu$, where $P(V)$ denotes pseudoscalar (vector) meson, can be written as

$$\begin{aligned}\mathcal{M} = -\frac{G_F}{\sqrt{2}} V_{q'b}\{&G_V \bar{l}\gamma_\mu(1-\gamma_5)\nu_l\langle(P,V)|\bar{q'}\gamma^\mu b|B\rangle - G_A\bar{l}\gamma_\mu(1-\gamma_5)\nu_l\langle(P,V)|\bar{q'}\gamma^\mu\gamma_5 b|B\rangle \\ &+ \tilde{G}_V\bar{l}\gamma_\mu(1+\gamma_5)\nu_l\langle(P,V)|\bar{q'}\gamma^\mu b|B\rangle - \tilde{G}_A\bar{l}\gamma_\mu(1+\gamma_5)\nu_l\langle(P,V)|\bar{q'}\gamma^\mu\gamma_5 b|B\rangle\}. \end{aligned} \tag{8}$$

The nonperturbative hadronic matrix elements in the decay amplitude can be parametrized in terms of various $B \to (P, V)$ transition form factors as follows:

$$\begin{aligned}\langle P(p')|\bar{q'}\gamma^\mu b|B(p)\rangle &= f_+(q^2)\left[(p+p')_\mu - \frac{M_B^2 - M_P^2}{q^2}q^\mu\right] + f_0(q^2)\frac{M_B^2 - M_P^2}{q^2}q^\mu, \\ \langle V(p',\epsilon^*)|\bar{q'}\gamma_\mu b|B(p)\rangle &= \frac{2iV(q^2)}{M_B + M_V}\varepsilon_{\mu\nu\rho\sigma}\epsilon^{*\nu}p^{\prime\rho}p^\sigma, \\ \langle V(p',\epsilon^*)|\bar{q'}\gamma_\mu\gamma_5 b|B(p)\rangle &= 2M_V A_0(q^2)\frac{\epsilon^*.q}{q^2}q_\mu + (M_B + M_V)A_1(q^2)\left[\epsilon^* - \frac{\epsilon^*.q}{q^2}q_\mu\right] \\ &\quad - A_2(q^2)\frac{\epsilon^*.q}{(M_B + M_V)}\left[(p+p')_\mu - \frac{M_B^2 - M_V^2}{q^2}q_\mu\right], \end{aligned} \tag{9}$$

where $q = p - p'$ is the momentum transfer. For the $B_s \to (K, K^*)$ and $B \to \pi$ transition form factors we use the formulas and the input values reported in Refs. [94–96]. The final expressions of $f_0(q^2)$ and $f_+(q^2)$ for $B_s \to Kl\nu$ decays are [94]

$$\begin{aligned} P_0(q^2)f_0(q^2) &= \sum_{k=1}^{3} b_k^{(0)}(z^k - z(0)^k) + \sum_{k=0}^{2} b_k^{(+)}\left[z(0)^k - (-1)^{k-3}\frac{k}{3}z(0)^3\right], \\ P_+(q^2)f_+(q^2) &= \sum_{k=0}^{2} b_k^{(+)}\left[z^k - (-1)^{k-3}\frac{k}{3}z^3\right]. \end{aligned} \tag{10}$$

Similarly, for the $B \to \pi$ transition form factors, the relevant expressions are [96]

$$f_+(q^2) = \frac{1}{(1 - \frac{q^2}{m_{B^*}^2})}\sum_{n=0}^{N_z-1} b_j^+\left[z^n - (-1)^{n-N_z}\frac{n}{N_z}z^{N_z}\right], \qquad f_0(q^2) = \sum_{n=0}^{N_z-1} b_j^0 z^n, \tag{11}$$

where $N_z = 4$ and

$$z(q^2) = \frac{\sqrt{t_+ - q^2} - \sqrt{t_+ - t_0}}{\sqrt{t_+ - q^2} + \sqrt{t_+ - t_0}}, \quad t_+ = (M_{B_{(s)}} + M_P)^2, \quad t_0 = (M_{B_{(s)}} + M_P)(\sqrt{M_{B_{(s)}}} - \sqrt{M_P})^2, \quad P_{0,+}(q^2) = 1 - \frac{q^2}{M_{0,+}^2}. \tag{12}$$

Here M_P refers to the mass of K or π meson, $M_0 = m_{B^*} = 5.6794(10)$ GeV and $M_+ = 5.32520(48)$ GeV represent the resonance masses. Again, for $B_s \to K^*$ form factors, the relevant expressions pertinent for our numerical analysis are [95]

$$F(t) = \frac{1}{P(t)}[a_0 + a_1 z], \tag{13}$$

where $t = q^2$ and $F(t)$ refers to the form factors V, A_0, A_1 and A_{12}, respectively. Here

$$A_{12}(q^2) = \frac{(M_{B_s} + M_{K^*})^2(M_{B_s}^2 - M_{K^*}^2 - q^2)A_1(q^2) - (t_+ - t)(t_- - t)A_2(q^2)}{16M_{B_s}M_{K^*}^2(M_{B_s} + M_{K^*})} \tag{14}$$

and

$$z(t, t_0) = \frac{\sqrt{t_+ - t} - \sqrt{t_+ - t_0}}{\sqrt{t_+ - t} + \sqrt{t_+ - t_0}}, \tag{15}$$

TABLE I. Theory inputs from PDG for $B_s \to Kl\nu$, $B_s \to K^* l\nu$ and $B \to \pi l\nu$.

Theory inputs from PDG [21]							
Parameters	Value	Parameters	Value	Parameters	Value	Parameters	Value
m_{B_s}	5.366 89	m_π	0.139 57	m_μ	0.105 6583715	τ_{B_0}	1.519×10^{-12}
m_K	0.4936 77	$m_b(\mu)$	4.18	$\lvert V_{cb}\rvert$	0.0409(11)	τ_{B_s}	1.505×10^{-12}
m_{K^*}	0.89176	$m_c(\mu)$	0.91	$\lvert V_{ub}\rvert$	0.003 61(22)	G_F	1.1663787×10^{-5}
m_{B^0}	5.279 55	m_τ	1.776 82				

where $t_0 = 12$ GeV and $t_\pm = (M_{B_s} \pm M_{K^*})^2$. We refer to Refs. [94–96] for all the omitted details.

Using the effective Lagrangian of Eq. (6), the three body differential decay distribution for the $B \to (P, V)l\nu$ decays can be written as

$$\frac{d\Gamma}{dq^2 d\cos\theta} = \frac{G_F^2 |V_{q'b}|^2 |\vec{P}_{(P,V)}|}{2^9 \pi^3 m_B^2} \left(1 - \frac{m_l^2}{q^2}\right) L_{\mu\nu} H^{\mu\nu}, \tag{16}$$

where $L_{\mu\nu}$ and $H^{\mu\nu}$ are the leptonic and hadronic current tensors. Here $|\vec{P}_{(P,V)}| = \sqrt{\lambda(m_B^2, m_{(P,V)}^2, q^2)}/2m_B$ with $\lambda(a,b,c) = a^2 + b^2 + c^2 - 2(ab + bc + ca)$ represent the three momentum vector of the outgoing meson. One can use the helicity techniques for the covariant contraction of $L_{\mu\nu}$ and $H^{\mu\nu}$, details of which can be found in Refs. [101,102]. We follow Ref. [61] and write the expression for differential decay distribution for $B \to (P, V)l\nu$ decays in terms of the helicity amplitudes H's and $\mathcal{A}$'s as follows:

$$\frac{d\Gamma^P}{dq^2 d\cos\theta} = 2N|\vec{P}_P| \Big\{ (G_V^2 + \tilde{G}_V^2) \Big[H_0^2 \sin^2\theta + \frac{m_l^2}{q^2} (H_0 \cos\theta - H_t)^2 \Big] \Big\}, \tag{17}$$

$$\frac{d\Gamma^V}{dq^2 d\cos\theta} = N|\vec{P}_V| \Big\{ 2\mathcal{A}_0^2 \sin^2\theta (G_A^2 + \tilde{G}_A^2) + \Big[(1 + \cos^2\theta) + \frac{m_l^2}{q^2} \sin^2\theta \Big] [\mathcal{A}_\parallel^2 (G_A^2 + \tilde{G}_A^2) + \mathcal{A}_\perp^2 (G_V^2 + \tilde{G}_V^2)] - 4\mathcal{A}_\parallel \mathcal{A}_\perp \cos\theta (G_A G_V - \tilde{G}_A \tilde{G}_V) + \frac{2m_l^2}{q^2} (G_A^2 + \tilde{G}_A^2) [\mathcal{A}_0 \cos\theta - \mathcal{A}_t]^2 \Big\}, \tag{18}$$

where θ is the angle between the $\vec{P}_{P,V}$ and lepton three momentum vector in the $l - \nu$ rest frame and

$$N = \frac{G_F^2 |V_{q'b}|^2 q^2}{256\pi^3 m_B^2} \left(1 - \frac{m_l^2}{q^2}\right)^2. \tag{19}$$

By performing the $\cos\theta$ integration in Eqs. (17) and (18), we get

$$\frac{d\Gamma^P}{dq^2} = \frac{8N|\vec{P}_P|}{3} (G_V^2 + \tilde{G}_V^2) \Big\{ H_0^2 \Big(1 + \frac{m_l^2}{2q^2}\Big) + \frac{3m_l^2}{2q^2} H_t^2 \Big\}, \tag{20}$$

$$\frac{d\Gamma^V}{dq^2} = \frac{8N|\vec{P}_V|}{3} \Big\{ \mathcal{A}_{AV}^2 + \frac{m_l^2}{2q^2} [\mathcal{A}_{AV}^2 + 3\mathcal{A}_t^2 (G_A^2 + \tilde{G}_A^2) + \tilde{\mathcal{A}}_{AV}^2] + \tilde{\mathcal{A}}_{AV}^2 \Big\}. \tag{21}$$

The SM equations can be obtained by setting $G_V = G_A = 1$ and $\tilde{G}_V = \tilde{G}_A = 0$. Explicit expressions of the helicity amplitudes H's and $\mathcal{A}$'s are presented in Ref. [61].

TABLE II. Form factor inputs for $B_s \to Kl\nu$, $B_s \to K^* l\nu$ and $B \to \pi l\nu$.

$B_s \to Kl\nu$ [94]			
Coefficients	Value	Coefficients	Value
$b_1^{(0)}$	0.315(129)	$b_0^{(+)}$	0.3680(214)
$b_2^{(0)}$	0.945(1.305)	$b_1^{(+)}$	−0.750(193)
$b_3^{(0)}$	2.391(4.671)	$b_2^{(+)}$	2.720(1.458)

$B_s \to K^* l\nu$ [95]			
$P(t; -42\ \text{MeV})V(t)$	Value	$P(t; -87\ \text{MeV})A_0(t)$	Value
a_0	0.322(48)	a_0	0.476(42)
a_1	−3.04(67)	a_1	−2.29(74)

$B_s \to K^* l\nu$ [95]			
$P(t; 350\ \text{MeV})A_1(t)$	Value	$P(t; 350\ \text{MeV})A_{12}(t)$	Value
a_0	0.2342 (122)	a_0	0.1954 (133)
a_1	0.100(174)	a_1	0.350(190)

$B \to \pi l\nu$ [96]			
Coefficients	Value	Coefficients	Value
b_0^0	0.510(19)	b_0^+	0.419(13)
b_1^0	−1.700(82)	b_1^+	−0.495(54)
b_2^0	1.53(19)	b_2^+	−0.43(13)
b_3^0	4.52(83)	b_3^+	0.22(31)

TABLE III. The first row reports the average values of the experimental inputs R_D, R_{D^*} [20], $R_{J/\Psi}$ [19] and R^l_π. The second row reports the 2σ range of the respective ratio of branching ratios.

	R_{D^*}	R_D	$R_{J/\Psi}$	R^l_π
Average values	$0.304 \pm 0.013 \pm 0.007$	$0.407 \pm 0.039 \pm 0.024$	$0.71 \pm 0.17 \pm 0.18$	0.698 ± 0.155
2σ range	[0.274, 0.334]	[0.315, 0.499]	[0.21, 1.21]	[0.388, 1.008]

The ratio of branching ratio is defined as

$$R = \frac{\mathcal{B}(B_{(s)} \to M\tau\nu)}{\mathcal{B}(B_{(s)} \to Ml\nu)}, \tag{22}$$

where $M = K, K^*, \pi$ and $l = \mu$. We also define various q^2 dependent observables such as differential branching ratio $D\mathrm{BR}(q^2)$, ratio of branching ratio $R(q^2)$, forward backward asymmetry $A^l_{FB}(q^2)$, polarization fraction of the charged lepton $P^l(q^2)$ and convexity parameter $C^l_F(q^2)$ for the decay modes as follows:

$$\begin{aligned}
\mathrm{DBR}(q^2) &= \frac{d\Gamma/dq^2}{\Gamma_{\mathrm{Tot}}}, \\
R(q^2) &= \frac{\mathcal{B}(B_{(s)} \to (P,V)\tau\nu)}{\mathcal{B}(B_{(s)} \to (P,V)l\nu)}, \\
A^{(P,V)}_{FB}(q^2) &= \frac{(\int^0_{-1} - \int^1_0) d\cos\theta \frac{d\Gamma^{(P,V)}}{dq^2 d\cos\theta}}{\frac{d\Gamma^{(P,V)}}{dq^2}}, \\
P^l_{(P,V)}(q^2) &= \frac{d\Gamma^{(P,V)}(-)/dq^2 - d\Gamma^{(P,V)}(+)/dq^2}{d\Gamma^{(P,V)}(+)/dq^2 + d\Gamma^{(P,V)}(-)/dq^2}, \\
C_F^{l^{(P,V)}}(q^2) &= \frac{1}{(d\Gamma^{(P,V)}/dq^2)} \frac{d^2}{d(\cos\theta)^2}\left[\frac{d\Gamma^{(P,V)}}{dq^2 d\cos\theta}\right],
\end{aligned} \tag{23}$$

where $d\Gamma^{(P,V)}(+)/dq^2$ and $d\Gamma^{(P,V)}(-)/dq^2$ represent the differential branching ratio of positive and negative helicity leptons, respectively. We also give predictions for the average values of the forward backward asymmetry of the charged lepton $\langle A^l_{FB}\rangle$, the convexity parameter $\langle C^l_F\rangle$, and the longitudinal polarization fraction of the charged lepton $\langle P^l\rangle$ which are calculated by separately integrating the numerator and the denominator over q^2. Although the τ momentum cannot be fully reconstructed from its decay process and the quantities such as $A^\tau_{FB}(q^2)$ and $P^\tau(q^2)$ are not directly accessible in the experiments, one can obtain this information from the subsequent decays of the τ lepton such as $\tau \to \pi\nu$, $\tau \to \rho\nu$ and $\tau \to l\nu\bar{\nu}$ [103]. It is worth mentioning that for the $B_q \to (P,V)\tau\nu$ decays, the forward backward asymmetry parameter $A^\tau_{FB}(q^2)$, the τ polarization fraction $P^\tau(q^2)$, and the convexity parameter $C^\tau_F(q^2)$ do not depend on V_L NP coupling if we assume that the NP effect is coming from new vector interactions V_L only. The NP dependency gets canceled in the ratio. On the other hand, although $A^\tau_{FB}(q^2)$ and $C^\tau_F(q^2)$ do not depend on $\tilde{V}_L$ NP coupling, the τ polarization fraction $P^\tau(q^2)$, however, does depend on this NP coupling. Measurement of the τ polarization fraction P^τ for these decay modes in future will be crucial to determine the exact nature of NP. Now let us proceed to the results and discussion.

TABLE IV. The central values and 1σ ranges of each observable for both μ and τ modes in SM are reported for $B_s \to Kl\nu$, $B_s \to K^*l\nu$ and $B \to \pi l\nu$ decays.

$B_s \to Kl\nu$		BR $\times 10^{-4}$	$\langle A^l_{FB}\rangle$	$\langle P^l\rangle$	$\langle C^l_F\rangle$	R_{B_sK}
μ mode	Central value	1.520	6.647×10^{-3}	0.982	−1.479	
	1σ range	[1.098, 2.053]	[0.006, 0.007]	[0.979, 0.984]	[−1.482, −1.478]	0.636
τ mode	Central value	0.966	0.284	0.105	−0.607	
	1σ range	[0.649, 1.392]	[0.262, 0.291]	[−0.035, 0.279]	[−0.711, −0.525]	[0.586, 0.688]
$B_s \to K^*l\nu$		BR $\times 10^{-4}$	$\langle A^l_{FB}\rangle$	$\langle P^l\rangle$	$\langle C^l_F\rangle$	$R_{B_sK^*}$
μ mode	Central value	3.259	−0.281	0.993	−0.417	
	1σ range	[2.501, 4.179]	[−0.342, −0.222]	[0.989, 0.995]	[−0.575, −0.247]	0.578
τ mode	Central value	1.884	−0.132	0.539	−0.105	
	1σ range	[1.449, 2.419]	[−0.203, −0.061]	[0.458, 0.603]	[−0.208, −0.007]	[0.539, 0.623]
$B \to \pi l\nu$		BR $\times 10^{-4}$	$\langle A^l_{FB}\rangle$	$\langle P^l\rangle$	$\langle C^l_F\rangle$	R_π
μ mode	Central value	1.369	4.678×10^{-3}	0.988	−1.486	
	1σ range	[1.030, 1.786]	[0.004, 0.006]	[0.981, 0.991]	[−1.489, −1.481]	0.641
τ mode	Central value	0.878	0.246	0.298	−0.737	
	1σ range	[0.690, 1.092]	[0.227, 0.262]	[0.195, 0.385]	[−0.781, −0.682]	[0.576, 0.725]

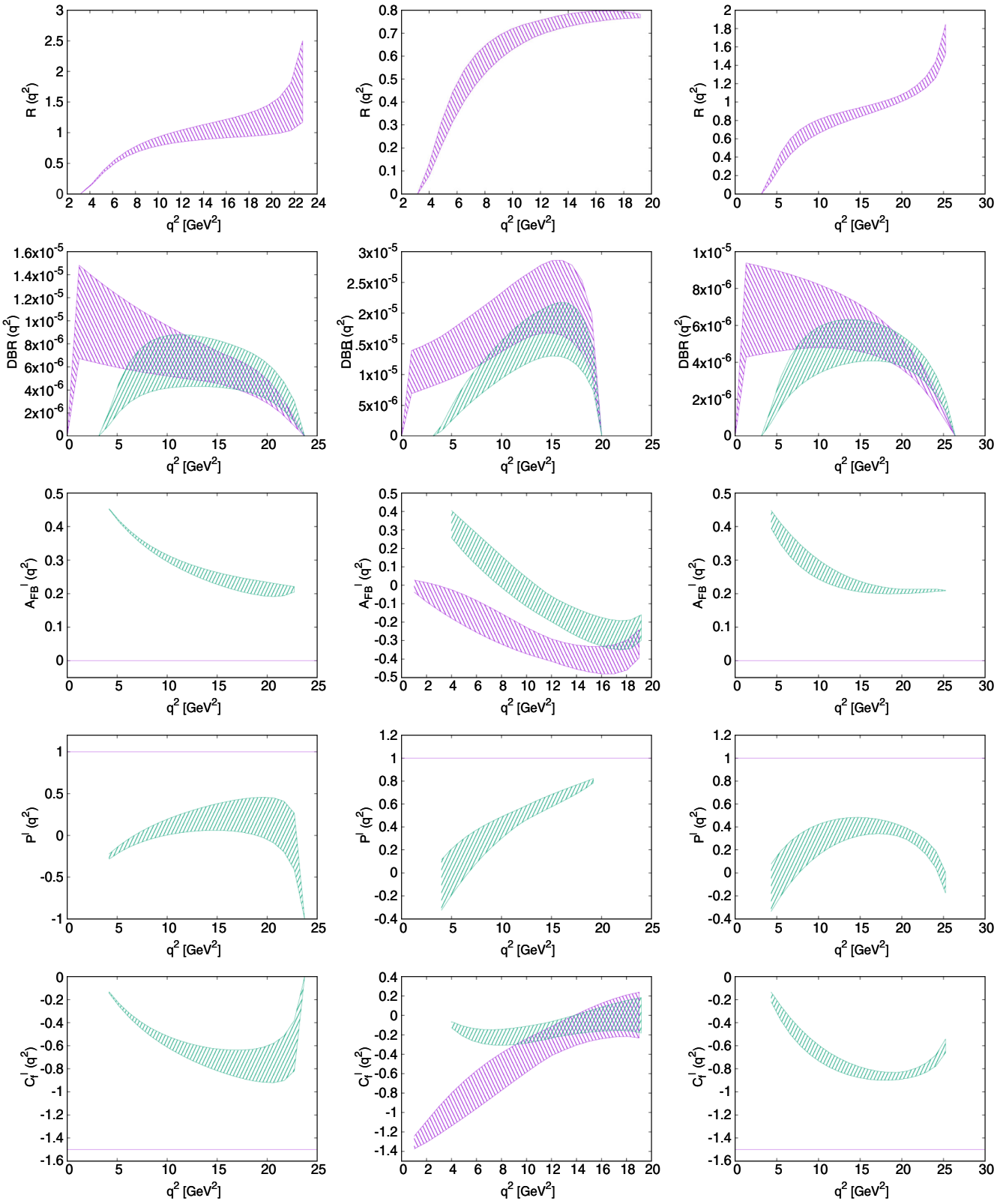

FIG. 1. q^2 dependent observables of $B_s \to Kl\nu$ (first column), $B_s \to K^* l\nu$ (second column) and $B \to \pi l\nu$ (third column) decays in the SM for the μ (violet) and τ (green) modes.

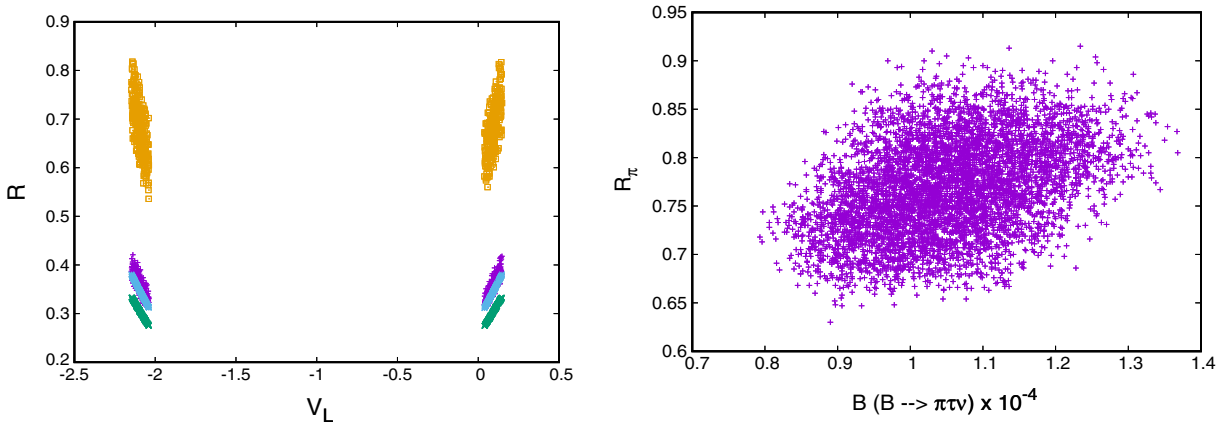

FIG. 2. In the left panel we show the allowed ranges in V_L NP coupling and the corresponding ranges in R_D (violet), R_{D^*} (green), $R_{J/\Psi}$ (blue), and R_π^l (yellow) once 2σ experimental constraint is imposed. The corresponding ranges in $\mathcal{B}(B \to \pi\tau\nu)$ and R_π are shown in the right panel.

III. RESULTS AND DISCUSSION

A. Input parameters

We first list out the theory input parameters in Table I that are relevant for our numerical analysis. The theory inputs such as mass of pseudoscalar mesons (K, π), vector meson (K^*), leptons (m_μ, m_τ), and quarks (m_b, m_c) are in GeV units. $m_b(\mu)$ and $m_c(\mu)$ refer to the masses of b and c quarks evaluated at $\mu = m_b$ renormalization scale. $|V_{cb}|$ and $|V_{ub}|$ are the corresponding CKM matrix elements for $b \to c$ and $b \to u$ transition decays. The Fermi coupling constant G_F and the lifetime of B^0 (τ_{B^0}) and B_s (τ_{B_s}) mesons are in the units of GeV^{-2} and seconds, respectively. The entries in Table II represent the respective form factor inputs for $B_s \to Kl\nu$ [94], $B_s \to K^* l\nu$ [95] and $B \to \pi l\nu$ [96] decays. For our analysis, we consider the uncertainties pertaining only to CKM matrix elements and form factor inputs. The number written within the parenthesis refers to the corresponding 1σ uncertainties. We also report the experimental input parameters R_D, R_{D^*}, $R_{J/\Psi}$ and R_π^l with their uncertainties measured by various B factory experiments such as *BABAR*, BELLE and LHCb in Table III. In our analysis, we added the statistical and systematic uncertainties in quadrature. The 2σ range of each of the experimental input parameters is also reported in Table III.

B. Standard model predictions

We first report in Table IV the SM predictions of various observables such as BR, ratio of branching ratio (R), forward backward asymmetry parameter ($\langle A_{FB}^l \rangle$), the polarization fraction of the charged lepton ($\langle P^l \rangle$), and the convexity parameter ($\langle C_F^l \rangle$) for the $B_s \to Kl\nu$, $B_s \to K^* l\nu$ and $B \to \pi l\nu$ decay modes, where l is either a μ lepton or a τ lepton, respectively. We find the branching ratio of all the decay modes to be of the order of 10^{-4}. We also give first prediction of various observables such as $\langle P^l \rangle$ and $\langle C_F^l \rangle$ for these decay modes. The central values reported in Table IV are calculated by considering the central values of the input parameters reported in Tables I and II, whereas, for the 1σ ranges, we perform a random scan over the theoretical inputs such as CKM matrix elements and the form factor inputs within 1σ of their central values. We observe that all the observables differ significantly while going from the μ mode to the τ mode. The forward backward asymmetry parameter $\langle A_{FB}^\mu \rangle$ for the $B_s \to K\mu\nu$ and $B \to \pi\mu\nu$ decays is vanishingly small, whereas $\langle P^\mu \rangle$ and $\langle C_F^\mu \rangle$ are nearly equal to 1 and -1.5, respectively. Although $\langle P^\mu \rangle$ for the $B_s \to K^*\mu\nu$ decays is quite similar to $B_s \to K\mu\nu$ and $B \to \pi\mu\nu$ decays, the $\langle A_{FB}^\mu \rangle$ and $\langle C_F^\mu \rangle$ for the $B_s \to K^*\mu\nu$ decays are quite different from the $B_s \to K\mu\nu$ and $B \to \pi\mu\nu$ decays. In Fig. 1, we show the q^2 dependency of all the observables for the μ mode and the τ mode, respectively. We notice that the q^2 behavior of all the observables for the μ mode is quite different from the corresponding τ mode. Again, the forward backward asymmetry parameter $A_{FB}^l(q^2)$, the τ polarization fraction $P^l(q^2)$, and the convexity parameter $C_F^l(q^2)$ for the $B_s \to K\mu\nu$ and $B \to \pi\mu\nu$ remain constant throughout the whole q^2 region. Similarly, for the $B_s \to K^*\mu\nu$ decays, we observe that the τ polarization fraction $P^l(q^2)$ remains constant in the whole q^2 region. This is quite obvious because in the $m_l \to 0$ limit, the q^2 dependency cancels in the ratio for these parameters. There is a zero crossing in the $A_{FB}^\tau(q^2)$ parameter for the $B_s \to K^*\tau\nu$ decays. However, we do not observe any zero crossing in the $A_{FB}^\tau(q^2)$ parameter for

TABLE V. Allowed ranges of each observable in the presence of V_L NP coupling of Fig. 2.

	R	$BR \times 10^{-4}$
$B_s \to K\tau\nu$	[0.644, 0.891]	[0.735, 1.746]
$B_s \to K^*\tau\nu$	[0.593, 0.804]	[1.684, 2.993]
$B \to \pi\tau\nu$	[0.630, 0.915]	[0.793, 1.368]

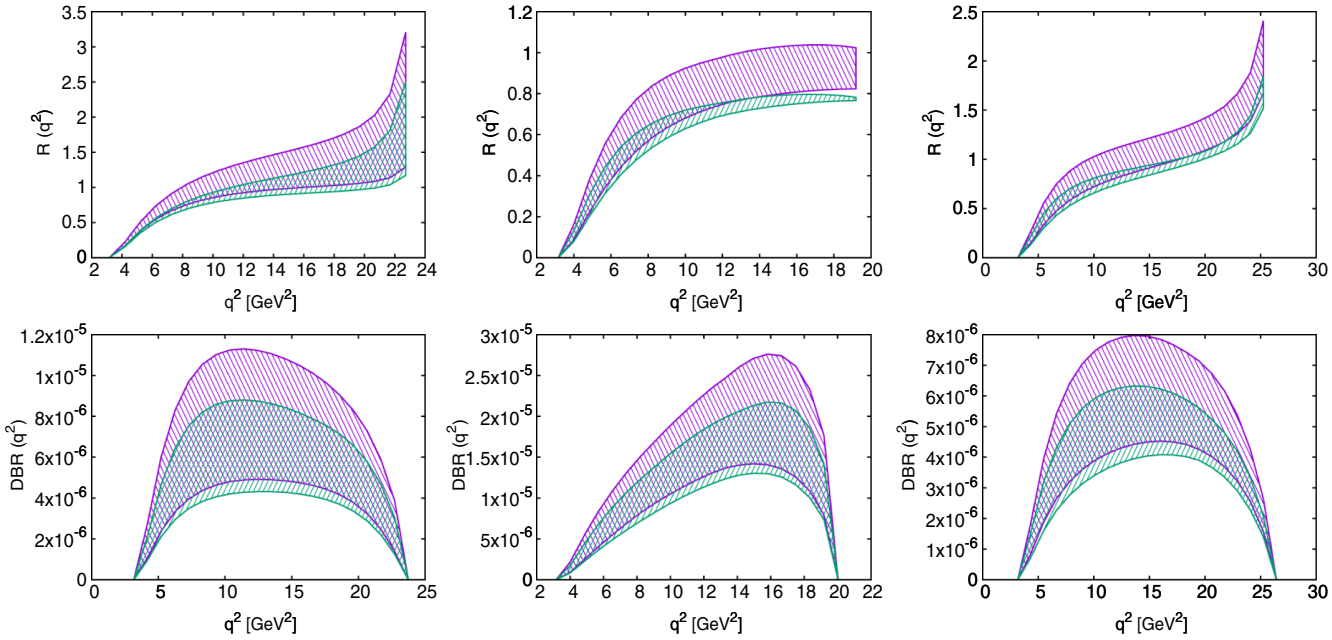

FIG. 3. Differential ratios $R(q^2)$ and differential branching ratios $\mathrm{DBR}(q^2)$ for $B_s \to K\tau\nu$ (first column), $B_s \to K^*\tau\nu$ (second column) and $B \to \pi\tau\nu$ (third column) decays using the V_L NP coupling of Fig. 2 are shown with a violet band, whereas the corresponding SM ranges are shown with a green band. The omitted plots such as $A_{FB}^{\tau}(q^2)$, $P^{\tau}(q^2)$ and $C_F^{\tau}(q^2)$ are not affected by V_L NP coupling.

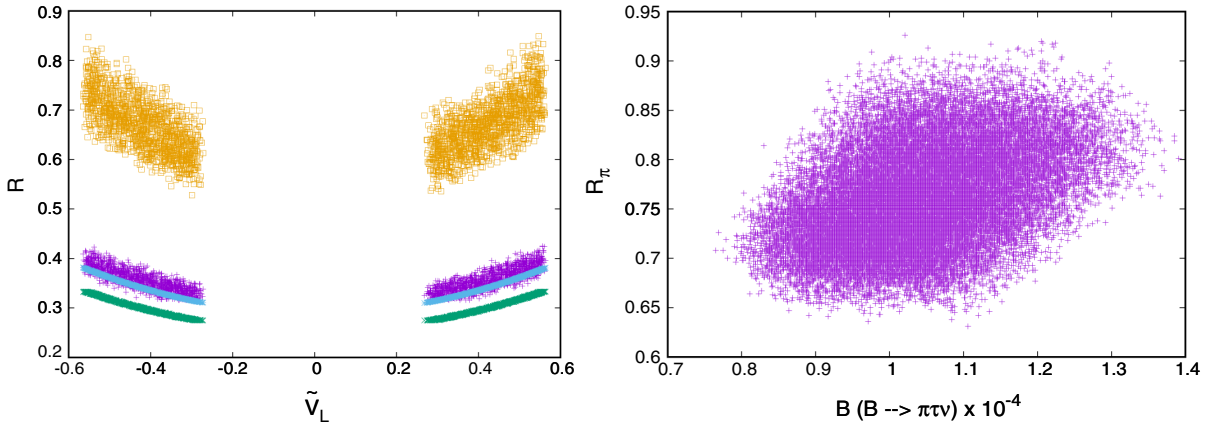

FIG. 4. In the left panel we show the allowed ranges in $\tilde{V}_L$ NP coupling and the corresponding ranges in R_D (violet), R_{D^*} (green), $R_{J/\Psi}$ (blue), and R_π^l (yellow) once 2σ experimental constraint is imposed. The corresponding ranges in $\mathcal{B}(B \to \pi\tau\nu)$ and R_π are shown in the right panel.

$B_s \to K\tau\nu$ and $B \to \pi\tau\nu$ decays. Similarly, we observe a zero crossing in the $P^{\tau}(q^2)$ observable for all the decay modes. We now proceed to discuss various NP scenarios.

TABLE VI. Allowed ranges of each observable in the presence of $\tilde{V}_L$ NP coupling of Fig. 4.

	R	$\mathrm{BR} \times 10^{-4}$	$\langle P^{\tau} \rangle$
$B_s \to K\tau\nu$	[0.638, 0.898]	[0.731, 1.774]	[−0.026, 0.217]
$B_s \to K^*\tau\nu$	[0.582, 0.802]	[1.579, 3.098]	[0.249, 0.513]
$B \to \pi\tau\nu$	[0.631, 0.926]	[0.765, 1.391]	[0.117, 0.315]

C. Beyond the SM predictions

We determine the impact of NP on various observables pertaining to $B_s \to (K, K^*)\tau\nu$ and $B \to \pi\tau\nu$ decays. To this end, we use an effective theory formalism in the presence of vector-type NP couplings and perform a model-dependent analysis based on anomalies present in R_D, R_{D^*}, $R_{J/\Psi}$, and R_π^l as well as the requirement $\mathcal{B}(B_c \to \tau\nu) \leq 10\%$ obtained from the LEP1 data [104]. It should, however, be mentioned that we assume the NP couplings to be quark flavor universal. This is, indeed, a strict model-dependent assumption. The branching ratio of taunic B_c decays put

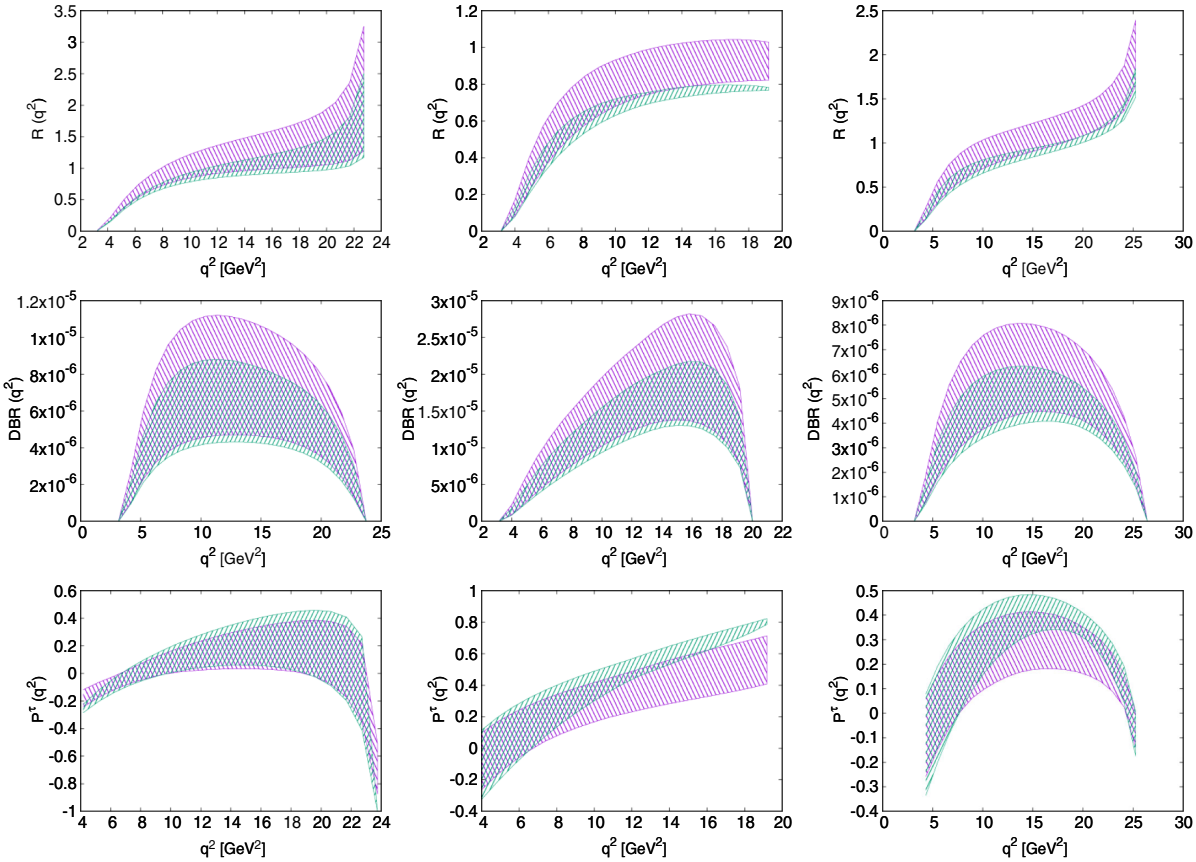

FIG. 5. Differential ratios $R(q^2)$, differential branching ratios $\mathrm{DBR}(q^2)$ and τ polarization fraction $P^\tau(q^2)$ for $B_s \to K\tau\nu$ (first column), $B_s \to K^*\tau\nu$ (second column) and $B \to \pi\tau\nu$ (third column) decays using the $\tilde{V}_L$ NP coupling of Fig. 4 are shown with a violet band, whereas the corresponding SM ranges are shown with a green band. The omitted plots such as $A_{FB}^\tau(q^2)$ and $C_F^\tau(q^2)$ are not affected by $\tilde{V}_L$ NP coupling.

a severe constraint on the scalar NP couplings [66]. Hence we do not consider scalar NP couplings in our present analysis. We consider only two different NP scenarios based on NP contribution coming from V_L and $\tilde{V}_L$ NP couplings. We consider only one NP WC at a time. We impose 2σ constraint coming from the measured value of R_D, R_{D^*}, $R_{J/\Psi}$, and R_π^l to determine the allowed NP parameter space. It should be mentioned that the NP contribution coming from V_R NP couplings cannot simultaneously explain the anomalies present in R_D, R_{D^*}, $R_{J/\Psi}$, and R_π^l within 2σ. Similarly, the NP contribution from $\tilde{V}_R$ NP coupling is exactly the same as the contribution coming from $\tilde{V}_L$ NP coupling. Hence, we omit the discussion related to these NP couplings.

1. Scenario I: For V_L NP coupling

In this scenario, we assume that NP contribution is coming only from V_L NP couplings. We vary V_L while keeping all other NP couplings zero. We show in the left panel of Fig. 2 the allowed range of V_L NP coupling once the 2σ constraints from the measured values of R_D, R_{D^*}, $R_{J/\Psi}$, and R_π^l are imposed. In the right panel, we show the ranges in $\mathcal{B}(B \to \pi\tau\nu)$ and R_π obtained using the allowed ranges of V_L NP coupling. Allowed ranges of $\mathcal{B}(B \to \pi\tau\nu)$ and R_π obtained in this scenario are compatible with the upper bound reported by Belle Collaboration. We also report the allowed ranges in the branching ratio and the ratio of branching ratios for the $B_s \to (K, K^*)\tau\nu$ and $B \to \pi\tau\nu$ decays in Table V. We see a significant deviation from the SM prediction in the branching ratios and the ratio of branching ratios with V_L NP couplings. Since the forward backward asymmetry parameter A_{FB}^τ, the τ polarization fraction P^τ, and the convexity parameter C_F^τ do not depend on V_L NP coupling, we do not observe any deviation from the SM prediction for these observables.

We show the q^2 dependence of differential branching ratio ($\mathrm{DBR}(q^2)$) and ratio of branching ratio $R(q^2)$ for the $B_s \to K\tau\nu$, $B_s \to K^*\tau\nu$ and $B \to \pi\tau\nu$ decays in Fig. 3. The SM range is shown with a green band, whereas the NP band obtained using the allowed values of V_L NP coupling from Fig. 2 is shown with a violet band. Again, as expected the remaining observables such as $A_{FB}^\tau(q^2)$, $P^\tau(q^2)$ and $C_F^\tau(q^2)$ exhibit no deviations from SM expectation as the V_L dependency cancels in the ratio.

2. Scenario II: For $\tilde{V}_L$ NP coupling

In this scenario, we vary only $\tilde{V}_L$ and set all other NP couplings to zero. This is to ensure that NP contribution is coming only from the vector NP operator that involves right handed neutrinos. The allowed NP parameter space is obtained by using a 2σ constraint coming from the measured values of R_D, R_{D^*}, $R_{J/\Psi}$, and R_π^l. This is to ensure that the resulting NP parameter space can simultaneously explain the anomalies present in R_D, R_{D^*}, $R_{J/\Psi}$, and R_π^l. We show in the left panel of Fig. 4 the allowed range of $\tilde{V}_L$ in this scenario. The corresponding ranges in $\mathcal{B}(B \to \pi\tau\nu)$ and R_π, shown in the right panel of Fig. 4, are compatible with the upper bound reported by Belle Collaboration. We also report the ranges of the branching ratio, ratio of branching ratios and τ polarization fraction for the $B_s \to K\tau\nu$, $B_s \to K^*\tau\nu$ and $B \to \pi\tau\nu$ decays in Table VI. We do not report the range of the forward backward asymmetry parameter $\langle A_{FB}^\tau \rangle$ and $\langle C_F^\tau \rangle$ since they do not depend on $\tilde{V}_L$ NP coupling. We see significant deviation from the SM expectation in the branching ratio, ratio of branching ratio, and τ polarization fraction for these decay modes in this scenario. Although the deviation observed in this scenario is quite similar to the deviation observed with V_L NP coupling, there is one subtle difference. Unlike scenario I, the τ polarization fraction P^τ does depend on $\tilde{V}_L$ NP coupling. Measurement of P^τ can, in principle, rule out either of these two scenarios.

In Fig. 5, we show the q^2 dependence of the ratio of branching ratio $R(q^2)$, differential branching ratio $\mathrm{DBR}(q^2)$ and τ polarization fraction $P^\tau(q^2)$ for the $B_s \to K\tau\nu$, $B_s \to K^*\tau\nu$ and $B \to \pi\tau\nu$ decays, respectively. The remaining observables such as forward backward asymmetry and convexity parameter are not affected by the $\tilde{V}_L$ NP coupling and hence we omit these results. The SM range is shown with a green band, whereas the band obtained by using the allowed $\tilde{V}_L$ NP coupling is shown with violet. It is evident that we do observe deviations in $R(q^2)$, $D\mathrm{BR}(q^2)$ and $P^\tau(q^2)$ from the SM predictions in the presence of $\tilde{V}_L$ NP coupling. It is worth mentioning that measurement of τ polarization fraction plays a crucial role in distinguishing between these two scenarios.

IV. CONCLUSION

Motivated by the anomalies present in R_D, R_{D^*}, $R_{J/\Psi}$, and R_π^l, we report the SM and beyond the SM predictions of various observables in $B_s \to K\tau\nu$, $B_s \to K^*\tau\nu$ and $B \to \pi\tau\nu$ decays in a model-dependent way. We perform a combined analysis of the $b \to c$ and $b \to u$ charged current interactions using an effective field theory approach in the presence of vector NP couplings alone. We start our analysis with the SM predictions by providing the central values and 1σ ranges of each observable for $B_s \to Kl\nu$, $B_s \to K^*l\nu$ and $B \to \pi l\nu$ decay modes. We give the predictions for both μ and τ modes, respectively. Considerable changes are observed while going from μ mode to τ mode. The branching ratio for each decay mode is of the order of 10^{-4}. We give the first prediction of various observables such as $\langle A_{FB}^l \rangle$, $\langle P^l \rangle$, and $\langle C_F^l \rangle$ within the SM and within various NP scenarios. It is also evident that the q^2 dependence of all the observables for the μ mode is quite different from that of the τ mode. We observe that some observables for the μ mode remain constant throughout the whole q^2 region.

For the NP analysis, we consider two NP scenarios with new vector-type operators that involve left handed as well as right handed neutrinos. We impose 2σ experimental constraints from the measured values of the ratio of branching ratios R_D, R_{D^*}, $R_{J/\Psi}$ and R_π^l and obtain the allowed ranges in the NP couplings that can simultaneously explain all these anomalies. We give prediction of various physical observables such as the branching ratio, ratio of branching ratios, forward backward asymmetry, lepton polarization and convexity parameter for the $B_s \to (K, K^*)\tau\nu$ and $B \to \pi\tau\nu$ decay modes in each scenario. The deviation from the SM prediction with V_L NP coupling is quite similar to the deviation observed with $\tilde{V}_L$ NP coupling. However, with $\tilde{V}_L$ NP coupling, there is deviation from the SM prediction in the τ polarization fraction P^τ for all the decay modes.

Although there is a hint of NP in semileptonic B decays mediated via charged current interactions, it is not yet confirmed. Study of $B_s \to Kl\nu$, $B_s \to K^*l\nu$ and $B \to \pi l\nu$ decay modes theoretically as well as experimentally is very well motivated as these can provide complementary information regarding NP. Again, it will have a direct consequence on predictions or the measurements of the CKM matrix element $|V_{ub}|$. The precise value of $|V_{ub}|$ will serve as an important step in revalidating the SM theory.

[1] J. A. Bailey *et al.* (MILC Collaboration), BD form factors at nonzero recoil and $|V_{cb}|$ from $2+1$-flavor lattice QCD, Phys. Rev. D **92**, 034506 (2015).

[2] H. Na, C. M. Bouchard, G. P. Lepage, C. Monahan, and J. Shigemitsu (HPQCD Collaboration), $B \to Dl\nu$ form factors at nonzero recoil and extraction of $|V_{cb}|$, Phys. Rev. D

92, 054510 (2015); Erratum, Phys. Rev. D 93, 119906(E) (2016).
[3] S. Aoki *et al.*, Review of lattice results concerning low-energy particle physics, Eur. Phys. J. C 77, 112 (2017).
[4] D. Bigi and P. Gambino, Revisiting $B \to D\ell\nu$, Phys. Rev. D 94, 094008 (2016).
[5] F. U. Bernlochner, Z. Ligeti, M. Papucci, and D. J. Robinson, Combined analysis of semileptonic B decays to D and D^*: $R(D^{(*)})$, $|V_{cb}|$, and new physics, Phys. Rev. D 95, 115008 (2017); Erratum 97, 059902(E) (2018).
[6] S. Jaiswal, S. Nandi, and S. K. Patra, Extraction of $|V_{cb}|$ from $B \to D^{(*)}\ell\nu_\ell$ and the Standard Model predictions of $R(D^{(*)})$, J. High Energy Phys. 12 (2017) 060.
[7] Y. M. Wang, Y. B. Wei, Y. L. Shen, and C. D. Lü, Perturbative corrections to B→D form factors in QCD, J. High Energy Phys. 06 (2017) 062.
[8] S. Fajfer, J. F. Kamenik, and I. Nisandzic, On the $B \to D^*\tau\bar{\nu}_\tau$ sensitivity to new physics, Phys. Rev. D 85, 094025 (2012).
[9] D. Bigi, P. Gambino, and S. Schacht, $R(D^*)$, $|V_{cb}|$, and the Heavy Quark Symmetry relations between form factors, J. High Energy Phys. 11 (2017) 061.
[10] M. A. Ivanov, J. G. Korner, and P. Santorelli, Semileptonic decays of B_c mesons into charmonium states in a relativistic quark model, Phys. Rev. D 71, 094006 (2005); Erratum, Phys. Rev. D 75, 019901(E) (2007).
[11] W. F. Wang, Y. Y. Fan, and Z. J. Xiao, Semileptonic decays $B_c \to (\eta_c, J/\Psi)l\nu$ in the perturbative QCD approach, Chin. Phys. C 37, 093102 (2013).
[12] R. Dutta and A. Bhol, $B_c \to (J/\psi, \eta_c)\tau\nu$ semileptonic decays within the standard model and beyond, Phys. Rev. D 96, 076001 (2017).
[13] T. D. Cohen, H. Lamm, and R. F. Lebed, Model-Independent Bounds on $R(J/\psi)$, arXiv:1807.02730.
[14] J. P. Lees *et al.* (*BABAR* Collaboration), Measurement of an excess of $\bar{B} \to D^{(*)}\tau^-\bar{\nu}_\tau$ decays and implications for charged Higgs bosons, Phys. Rev. D 88, 072012 (2013).
[15] M. Huschle *et al.* (Belle Collaboration), Measurement of the branching ratio of $\bar{B} \to D^{(*)}\tau^-\bar{\nu}_\tau$ relative to $\bar{B} \to D^{(*)}\ell^-\bar{\nu}_\ell$ decays with hadronic tagging at Belle, Phys. Rev. D 92, 072014 (2015).
[16] Y. Sato *et al.* (Belle Collaboration), Measurement of the branching ratio of $\bar{B}^0 \to D^{*+}\tau^-\bar{\nu}_\tau$ relative to $\bar{B}^0 \to D^{*+}\ell^-\bar{\nu}_\ell$ decays with a semileptonic tagging method, Phys. Rev. D 94, 072007 (2016).
[17] S. Hirose *et al.* (Belle Collaboration), Measurement of the τ Lepton Polarization and $R(D^*)$ in the Decay $\bar{B} \to D^*\tau^-\bar{\nu}_\tau$, Phys. Rev. Lett. 118, 211801 (2017).
[18] R. Aaij *et al.* (LHCb Collaboration), Measurement of the Ratio of Branching Fractions $\mathcal{B}(\bar{B}^0 \to D^{*+}\tau^-\bar{\nu}_\tau)/\mathcal{B}(\bar{B}^0 \to D^{*+}\mu^-\bar{\nu}_\mu)$, Phys. Rev. Lett. 115, 111803 (2015); Erratum, Phys. Rev. Lett. 115, 159901(E) (2015).
[19] R. Aaij *et al.* (LHCb Collaboration), Measurement of the Ratio of Branching Fractions $\mathcal{B}(B_c^+ \to J/\psi\tau^+\nu_\tau)/\mathcal{B}(B_c^+ \to J/\psi\mu^+\nu_\mu)$, Phys. Rev. Lett. 120, 121801 (2018).
[20] Y. Amhis *et al.* (HFLAV Collaboration), Averages of b-hadron, c-hadron, and τ-lepton properties as of summer 2016, Eur. Phys. J. C 77, 895 (2017).
[21] C. Patrignani *et al.* (Particle Data Group Collaboration), Review of particle physics, Chin. Phys. C 40, 100001 (2016).
[22] J. P. Lees *et al.* (*BABAR* Collaboration), Evidence of $B^+ \to \tau^+\nu$ decays with hadronic B tags, Phys. Rev. D 88, 031102 (2013).
[23] B. Aubert *et al.* (*BABAR* Collaboration), Search for $B^+ \to \ell^+\nu_\ell$ recoiling against $B^- \to D^0\ell^-\bar{\nu}X$, Phys. Rev. D 81, 051101 (2010).
[24] I. Adachi *et al.* (Belle Collaboration), Evidence for $B^- \to \tau^-\bar{\nu}_\tau$ with a Hadronic Tagging Method Using the Full Data Sample of Belle, Phys. Rev. Lett. 110, 131801 (2013).
[25] B. Kronenbitter *et al.* (Belle Collaboration), Measurement of the branching fraction of $B^+ \to \tau^+\nu_\tau$ decays with the semileptonic tagging method, Phys. Rev. D 92, 051102 (2015).
[26] J. Charles *et al.*, Predictions of selected flavor observables within the standard model, Phys. Rev. D 84, 033005 (2011).
[27] J. Charles, A. Höcker, H. Lacker, S. Laplace, F. R. Diberder, J. Malclés, J. Ocariz, M. Pivk, and L. Roos (CKMfitter Group Collaboration), *CP* violation and the CKM matrix: Assessing the impact of the asymmetric B factories, Eur. Phys. J. C 41, 1 (2005).
[28] M. Bona *et al.* (UTfit Collaboration), An improved standard model prediction of $BR(B \to \tau\nu)$ and its implications for new physics, Phys. Lett. B 687, 61 (2010).
[29] H. Ha *et al.* (Belle Collaboration), Measurement of the decay $B^0 \to \pi^-\ell^+\nu$ and determination of $|V_{ub}|$, Phys. Rev. D 83, 071101 (2011).
[30] T. Hokuue *et al.* (Belle Collaboration), Measurements of branching fractions and q^2 distributions for $B \to \pi\ell\nu$ and $B \to \rho\ell\nu$ decays with $B \to D^{(*)}\ell\nu$ decay tagging, Phys. Lett. B 648, 139 (2007).
[31] I. Adachi *et al.* (Belle Collaboration), Measurement of exclusive B→X(u) l nu decays using full-reconstruction tagging at Belle, arXiv:0812.1414.
[32] P. del Amo Sanchez *et al.* (*BABAR* Collaboration), Study of $B \to \pi\ell\nu$ and $B \to \rho\ell\nu$ decays and determination of $|V_{ub}|$, Phys. Rev. D 83, 032007 (2011).
[33] B. Aubert *et al.* (*BABAR* Collaboration), Measurement of the $B \to \pi\ell\nu$ Branching Fraction and Determination of $|V_{ub}|$ with Tagged B Mesons, Phys. Rev. Lett. 97, 211801 (2006).
[34] B. Aubert *et al.* (*BABAR* Collaboration), Measurement of the $B^0 \to \pi^-\ell^+\nu$ Form-Factor Shape and Branching Fraction, and Determination of $|V_{ub}|$ with a Loose Neutrino Reconstruction Technique, Phys. Rev. Lett. 98, 091801 (2007).
[35] B. Aubert *et al.* (*BABAR* Collaboration), Measurements of $B \to \{\pi, \eta, \eta'\}\ell\nu_\ell$ Branching Fractions and Determination of $|V_{ub}|$ with Semileptonically Tagged B Mesons, Phys. Rev. Lett. 101, 081801 (2008).
[36] N. E. Adam *et al.* (CLEO Collaboration), A Study of Exclusive Charmless Semileptonic B Decay and $|V_{ub}|$, Phys. Rev. Lett. 99, 041802 (2007).

[37] P. Hamer *et al.* (Belle Collaboration), Search for $B^0 \to \pi^-\tau^+\nu_\tau$ with hadronic tagging at Belle, Phys. Rev. D **93**, 032007 (2016).

[38] F. U. Bernlochner, $B \to \pi\tau\bar{\nu}_\tau$ decay in the context of type II 2HDM, Phys. Rev. D **92**, 115019 (2015).

[39] S. Fajfer, J. F. Kamenik, I. Nisandzic, and J. Zupan, Implications of Lepton Flavor Universality Violations in B Decays, Phys. Rev. Lett. **109**, 161801 (2012).

[40] M. Tanaka, Charged Higgs effects on exclusive semi-tauonic B decays, Z. Phys. C **67**, 321 (1995).

[41] U. Nierste, S. Trine, and S. Westhoff, Charged-Higgs effects in a new $B \to D_{\tau\nu_\tau}$ differential decay distribution, Phys. Rev. D **78**, 015006 (2008).

[42] T. Miki, T. Miura, and M. Tanaka, Effects of charged Higgs boson and QCD corrections in $\bar{B} \to D_{\tau\bar{\nu}_\tau}$, arXiv: hep-ph/0210051.

[43] A. Wahab El Kaffas, P. Osland, and O. M. Ogreid, Constraining the two-Higgs-doublet-model parameter space, Phys. Rev. D **76**, 095001 (2007).

[44] A. G. Akeroyd and S. Recksiegel, The effect of $H^\pm$ on $B^\pm \to T^\pm V_T$ and $B^\pm \to \mu^\pm V_\mu$, J. Phys. G **29**, 2311 (2003).

[45] O. Deschamps, S. Descotes-Genon, S. Monteil, V. Niess, S. T'Jampens, and V. Tisserand, The two Higgs doublet of type II facing flavor physics data, Phys. Rev. D **82**, 073012 (2010).

[46] G. Blankenburg and G. Isidori, $B \to \tau\nu$ in two-Higgs-doublet models with MFV, Eur. Phys. J. Plus **127**, 85 (2012).

[47] G. D'Ambrosio, G. F. Giudice, G. Isidori, and A. Strumia, Minimal flavor violation: An effective field theory approach, Nucl. Phys. **B645**, 155 (2002).

[48] A. J. Buras, M. V. Carlucci, S. Gori, and G. Isidori, Higgs-mediated FCNCs: Natural flavor conservation vs minimal Flavor violation, J. High Energy Phys. 10 (2010) 009.

[49] A. Pich and P. Tuzon, Yukawa alignment in the two-Higgs-doublet model, Phys. Rev. D **80**, 091702 (2009).

[50] A. Crivellin, C. Greub, and A. Kokulu, Explaining $B \to D\tau\nu$, $B \to D^*\tau\nu$ and $B \to \tau\nu$ in a 2HDM of type III, Phys. Rev. D **86**, 054014 (2012).

[51] A. Datta, M. Duraisamy, and D. Ghosh, Diagnosing new physics in $b \to c\tau\nu_\tau$ decays in the light of the recent *BABAR* result, Phys. Rev. D **86**, 034027 (2012).

[52] M. Duraisamy and A. Datta, The full $B \to D^*\tau^-\bar{\nu}_\tau$ angular distribution and CP violating triple products, J. High Energy Phys. 09 (2013) 059.

[53] M. Duraisamy, P. Sharma, and A. Datta, Azimuthal $B \to D^*\tau^-\bar{\nu}_\tau$ angular distribution with tensor operators, Phys. Rev. D **90**, 074013 (2014).

[54] M. Jung, A. Pich, and P. Tuzon, Charged-Higgs phenomenology in the aligned two-Higgs-doublet model, J. High Energy Phys. 11 (2010) 003.

[55] P. Biancofiore, P. Colangelo, and F. De Fazio, On the anomalous enhancement observed in $B \to D^{(*)}\tau\bar{\nu}_\tau$ decays, Phys. Rev. D **87**, 074010 (2013).

[56] A. Celis, M. Jung, X. Q. Li, and A. Pich, Sensitivity to charged scalars in $\boldsymbol{B \to D^{(*)}\tau\nu_\tau}$ and $\boldsymbol{B \to \tau\nu_\tau}$ decays, J. High Energy Phys. 01 (2013) 054.

[57] B. Bhattacharya, A. Datta, D. London, and S. Shivashankara, Simultaneous explanation of the R_K and $R(D^{(*)})$ puzzles, Phys. Lett. B **742**, 370 (2015).

[58] B. Bhattacharya, A. Datta, J. P. Guvin, D. London, and R. Watanabe, Simultaneous explanation of the R_K and $R_{D^{(*)}}$ puzzles: A model analysis, J. High Energy Phys. 01 (2017) 015.

[59] A. Crivellin, Effects of right-handed charged currents on the determinations of $|V_{ub}| \times and \times |V_{cb}|$, Phys. Rev. D **81**, 031301 (2010).

[60] X. G. He and G. Valencia, B decays with τ leptons in nonuniversal left-right models, Phys. Rev. D **87**, 014014 (2013).

[61] R. Dutta, A. Bhol, and A. K. Giri, Effective theory approach to new physics in $b \to u$ and $b \to c$ leptonic and semileptonic decays, Phys. Rev. D **88**, 114023 (2013).

[62] N. G. Deshpande and X. G. He, Consequences of R-parity violating interactions for anomalies in $\bar{B} \to D^{(*)}\tau\bar{\nu}$ and $b \to s\mu^+\mu^-$, Eur. Phys. J. C **77**, 134 (2017).

[63] X. Q. Li, Y. D. Yang, and X. Zhang, Revisiting the one leptoquark solution to the $R(D^{(})})$ anomalies and its phenomenological implications, J. High Energy Phys. 08 (2016) 054.

[64] M. Tanaka and R. Watanabe, New physics contributions in $B \to \pi\tau\bar{\nu}$ and $B \to \tau\bar{\nu}$, Prog. Theor. Exp. Phys. **2017**, 013B05 (2017).

[65] D. Bardhan, P. Byakti, and D. Ghosh, A closer look at the R_D and R_{D^*} anomalies, J. High Energy Phys. 01 (2017) 125.

[66] R. Alonso, B. Grinstein, and J. Martin Camalich, Lifetime of $B_{\bar{c}}$ Mesons Constrains Explanations for Anomalies in $B \to D^{(*)}\tau\nu$, Phys. Rev. Lett. **118**, 081802 (2017).

[67] A. K. Alok, D. Kumar, S. Kumbhakar, and S. U. Sankar, D^* polarization as a probe to discriminate new physics in $\bar{B} \to D^*\tau\bar{\nu}$, Phys. Rev. D **95**, 115038 (2017).

[68] D. Du, A. X. El-Khadra, S. Gottlieb, A. S. Kronfeld, J. Laiho, E. Lunghi, R. S. Van de Water, and R. Zhou, Phenomenology of semileptonic B-meson decays with form factors from lattice QCD, Phys. Rev. D **93**, 034005 (2016).

[69] A. Soffer, B-meson decays into final states with a lepton, Mod. Phys. Lett. A **29**, 1430007 (2014).

[70] M. Bordone, G. Isidori, and D. van Dyk, Impact of leptonic τ decays on the distribution of $B \to P\mu\bar{\nu}$ decays, Eur. Phys. J. C **76**, 360 (2016).

[71] M. A. Ivanov, J. G. Krner, and C. T. Tran, Looking for new physics in leptonic and semileptonic decays of B-meson, Phys. Part. Nucl. Lett. **14**, 669 (2017).

[72] M. A. Ivanov, J. G. Krner, and C. T. Tran, Analyzing new physics in the decays $\bar{B}^0 \to D^{(*)}\tau^-\bar{\nu}_\tau$ with form factors obtained from the covariant quark model, Phys. Rev. D **94**, 094028 (2016).

[73] S. M. Boucenna, A. Celis, J. Fuentes-Martin, A. Vicente, and J. Virto, Phenomenology of an $SU(2) \times SU(2) \times U(1)$ model with lepton-flavor nonuniversality, J. High Energy Phys. 12 (2016) 059.

[74] S. M. Boucenna, A. Celis, J. Fuentes-Martin, A. Vicente, and J. Virto, Non-Abelian gauge extensions for B-decay anomalies, Phys. Lett. B **760**, 214 (2016).

[75] W. S. Hou, Enhanced charged Higgs boson effects in $B^- \to \tau\bar{\nu}, \mu\bar{\nu}$ and $b \to \tau\bar{\nu} + X$, Phys. Rev. D **48**, 2342 (1993).

[76] G. Ciezarek, M. Franco Sevilla, B. Hamilton, R. Kowalewski, T. Kuhr, V. Lth, and Y. Sato, A challenge to lepton universality in B meson decays, Nature (London) **546**, 227 (2017).
[77] L. Dhargyal, Explaining the observed deviation in $R(D^{(*)})$ and $Br(B \to \tau\nu_\tau)$ in an anomalous 2HDM, Springer Proc. Phys. **203**, 681 (2018).
[78] P. Colangelo and F. De Fazio, Scrutinizing $\bar{B} \to D^*(D\pi)\ell^-\bar{\nu}_\ell$ and $\bar{B} \to D^*(D\gamma)\ell^-\bar{\nu}_\ell$ in search of new physics footprints, J. High Energy Phys. 06 (2018) 082.
[79] R. Dutta and A. Bhol, $b \to (c, u), \tau\nu$ leptonic and semileptonic decays within an effective field theory approach, Phys. Rev. D **96**, 036012 (2017).
[80] G. Buchalla, A. J. Buras, and M. E. Lautenbacher, Weak decays beyond leading logarithms, Rev. Mod. Phys. **68**, 1125 (1996).
[81] S. Nandi, S. K. Patra, and A. Soni, Correlating new physics signals in $B \to D^{(*)}\tau\nu_\tau$ with $B \to \tau\nu_\tau$, arXiv:1605.07191.
[82] W. Altmannshofer, P. S. Bhupal Dev, and A. Soni, $R_{D^{(*)}}$ anomaly: A possible hint for natural supersymmetry with R-parity violation, Phys. Rev. D **96**, 095010 (2017).
[83] S. Iguro and K. Tobe, $R(D^{(*)})$ in a general two-Higgs-doublet model, Nucl. Phys. **B925**, 560 (2017).
[84] R. Watanabe, New physics effect on $B_c \to J/\psi\tau\bar{\nu}$ in relation to the $R_{D^{(*)}}$ anomaly, Phys. Lett. B **776**, 5 (2018).
[85] R. Dutta, Exploring R_D, R_{D^*} and $R_{J/\Psi}$ anomalies, arXiv:1710.00351.
[86] S. Bhattacharya, S. Nandi, and S. K. Patra, Looking for possible new physics in $B \to D^{(*)}\tau\nu_\tau$ in light of recent data, Phys. Rev. D **95**, 075012 (2017).
[87] R. Dutta and N. Rajeev, Signature of lepton flavor universality violation in $B_s \to D_s\tau\nu$ semileptonic decays, Phys. Rev. D **97**, 095045 (2018).
[88] N. Assad, B. Fornal, and B. Grinstein, Baryon number and lepton universality violation in leptoquark and diquark models, Phys. Lett. B **777**, 324 (2018).
[89] Z. R. Huang, Y. Li, C. D. Lu, M. A. Paracha, and C. Wang, Footprints of new physics in $b \to c\tau\nu$ transitions, arXiv:1808.03565.
[90] R. N. Faustov and V. O. Galkin, Charmless weak B_s decays in the relativistic quark model, Phys. Rev. D **87**, 094028 (2013).
[91] W. F. Wang and Z. J. Xiao, The semileptonic decays $B/B_s \to (\pi, K)(\ell^+\ell^-, \ell\nu, \nu\bar{\nu})$ in the perturbative QCD approach beyond the leading order, Phys. Rev. D **86**, 114025 (2012).
[92] C. H. Chen and C. Q. Geng, Charged Higgs on $B^- \to T\bar{\nu}_T$ and $B^- \to P(V)\ell_{\bar{\nu}_\ell}$, J. High Energy Phys. 10 (2006) 053.
[93] A. Khodjamirian, T. Mannel, N. Offen, and Y.-M. Wang, $B \to \pi\ell\nu_l$ width and $|V_{ub}|$ from QCD light-cone sum rules, Phys. Rev. D **83**, 094031 (2011).
[94] C. M. Bouchard, G. P. Lepage, C. Monahan, H. Na, and J. Shigemitsu, $B_s \to K\ell\nu$ form factors from lattice QCD, Phys. Rev. D **90**, 054506 (2014).
[95] R. R. Horgan, Z. Liu, S. Meinel, and M. Wingate, Lattice QCD calculation of form factors describing the rare decays $B \to K^*\ell^+\ell^-$ and $B_s \to \phi\ell^+\ell^-$, Phys. Rev. D **89**, 094501 (2014).
[96] J. A. Bailey *et al.* (Fermilab Lattice and MILC Collaborations), $|V_{ub}|$ from $B \to \pi\ell\nu$ decays and $(2+1)$-flavor lattice QCD, Phys. Rev. D **92**, 014024 (2015).
[97] S. Sahoo, A. Ray, and R. Mohanta, Model-independent investigation of rare semileptonic $b \to ul\bar{\nu}_l$ decay processes, Phys. Rev. D **96**, 115017 (2017).
[98] X. W. Kang, T. Luo, Y. Zhang, L. Y. Dai, and C. Wang, Semileptonic B and B_s decays involving scalar and axial-vector mesons, arXiv:1808.02432.
[99] V. Cirigliano, J. Jenkins, and M. Gonzalez-Alonso, Semileptonic decays of light quarks beyond the standard model, Nucl. Phys. **B830**, 95 (2010).
[100] T. Bhattacharya, V. Cirigliano, S. D. Cohen, A. Filipuzzi, M. Gonzalez-Alonso, M. L. Graesser, R. Gupta, and H. W. Lin, Probing novel scalar and tensor interactions from (ultra)cold neutrons to the LHC, Phys. Rev. D **85**, 054512 (2012).
[101] J. G. Korner and G. A. Schuler, Exclusive semileptonic heavy meson decays including lepton mass effects, Z. Phys. C **46**, 93 (1990).
[102] A. Kadeer, J. G. Korner, and U. Moosbrugger, Helicity analysis of semileptonic hyperon decays including lepton mass effects, Eur. Phys. J. C **59**, 27 (2009).
[103] R. Alonso, J. Martin Camalich, and S. Westhoff, Tau properties in $B \to D\tau\nu$ from visible final-state kinematics, Phys. Rev. D **95**, 093006 (2017).
[104] A. G. Akeroyd and C. H. Chen, Constraint on the branching ratio of $B_c \to \tau\bar{\nu}$ from LEP1 and consequences for $R(D^{(*)})$ anomaly, Phys. Rev. D **96**, 075011 (2017).